Available online at www.sciencedirect.com
SCIENCE DIRECT

Journal of Sound and Vibration 268 (2003) 699–716

JOURNAL OF SOUND AND VIBRATION

www.elsevier.com/locate/jsvi

A time-domain approach for damage detection in beam structures using vibration data with a moving oscillator as an excitation source

Luna Majumder, C.S. Manohar*

Department of Civil Engineering, Indian Institute of Science, Bangalore 560 012, India

Received 29 April 2002; accepted 21 November 2002

Abstract

The problem of detecting local/distributed change of stiffness in bridge structures using ambient vibration data is considered. The vibration induced by a vehicle moving on the bridge is taken to be the excitation source. A validated finite element model for the bridge structure in its undamaged state is assumed to be available. Alterations to be made to this initial model, to reflect the changes in bridge behaviour due to occurrence of damage, are determined using a time-domain approach. The study takes into account complicating features arising out of dynamic interactions between vehicle and the bridge, bridge deck unevenness, spatial incompleteness of measured data and presence of measurement noise. The inclusion of vehicle inertia, stiffness and damping characteristics into the analysis makes the system time variant, which, in turn, necessitates treatment of the damage detection problem in time domain. The efficacy of the procedures developed is demonstrated by considering detection of localized/distributed damages in a beam-moving oscillator model using synthetically generated vibration data.

1. Introduction

The occurrence of damage in a structure produces changes in its global dynamic characteristics such as its natural frequencies, mode shapes, modal damping, modal participation factors, impulse response and frequency response functions. An understanding of these changes can lead to the detection, location, and the characterization of the extent of the damage. Such studies currently form the subject of active research in the field of aerospace, mechanical and civil structural health monitoring. In civil engineering applications, these studies are of immediate

*Corresponding author. Tel.: +91-80-309-2667; fax: +91-80-360-0404.
E-mail addresses: luna@civil.iisc.ernet.in (L. Majumder), manohar@civil.iisc.ernet.in (C.S. Manohar).

0022-460X/03/$ - see front matter
doi:10.1016/S0022-460X(02)01555-9

relevance to the health monitoring of ageing civil infrastructures, such as buildings and bridges, in assessment of these structures after natural disasters, and in evaluation of effectiveness of retrofitting/repair measures. The essential underlying principle here is to compare the structural behaviour in the damaged and undamaged states. If interest is focussed on determining the location of damage and the extent of damage, the analyst would require a satisfactory model for the structure in its undamaged state. The construction of such reliable models can be achieved by comparing experimentally obtained data on structure in its initial state with corresponding predictions made from an initial mathematical model [1]. The developments in the field of structural damage detection using vibration data have been recently reviewed by several authors. Thus Farrar et al. [2] have outlined steps for implementing structural health monitoring programme using vibration data. They have also discussed the damage detection problem as a problem in statistical pattern recognition. Doebling et al. [3,4] have presented comprehensive review of literature mainly focusing on frequency-domain methods for damage detection in linear structures. The relationship between model updating methods and damage detection problem has been explored by He [5]. A discussion on methods of damage detection and location using natural frequency changes has been presented by Salawu [6]. Staszewski [7] has reviewed the literature related to the use of wavelets in structural damage detection problems.

Some recent studies on the use of vibration data in damage assessment of civil structures are briefly described in the following. Mazurek and DeWolf [8] conducted theoretical and laboratory experimental studies on simple two-span girders under moving loads to study structural deterioration by vibration signature analysis. Structural damages were artificially introduced by release of supports and insertion of cracks. Hearn and Testa [9] conducted studies on fatigue damaged welded steel building frames and wire ropes with saw-cuts and studied the changes in the frequency spectra caused due to damage. Yao et al. [10] considered the redistribution of energy upon the occurrence of damage and discussed the concept of strain mode shape in characterizing the damage. Alampalli and Fu [11] and Alampalli et al. [12] conducted laboratory and field studies on bridge structures to investigate the feasibility of measuring bridge vibration for inspection and evaluation. These studies focused on sensitivity of measured modal parameters to damage. Cross diagnosis using multiple signatures involving natural frequencies, mode shapes, modal assurance criteria and co-ordinate modal assurance criteria was shown to be necessary to detect the damages. Casas and Aparicio [13] studied concrete bridge structures and investigated dynamic response as an inspection tool to assess bearing conditions and girder cracking. Their study showed the need to investigate more than one natural frequency and also to determine mode shapes in order that the damage could be successfully detected and located. Issues related to mismatch between measured and modelled degrees of freedom (d.o.f.'s) in large-scale building frame structures have been examined by Koh [14] in the context of damage detection problems. Liu [15] examined the identifiability of inverse problems and influence of input errors on identification process in the context of identification and damage detection in truss structures. Combined experimental and finite element modelling studies has been carried out by Chen et al. [16] on steel channel beams, to detect reduction in load carrying capacity using dynamic response. Law et al. [17,18] measured vibrational response of concrete bridge deck models when loaded to destruction at different stages of cracking and spalling. The possible absence of base line models for existing structures and its consequence on problem of damage detection has been noted by Topole and Stubbs [19]. These authors developed a method to characterize the damage from the data on modal characteristics of the damaged structure. The study by Salawu and Williams [20] describes full-scale vibration tests conducted before and after structural repairs on a multi-span RCC highway bridge. Correlations between repair works and changes in dynamic characteristics of the bridge were studied. Waheb and Roeck [21] describe the results of field vibration tests on three concrete bridges with a view to correlate finite element models with test results. The use of residual force vector and a sensitivity analysis has been made by Kosmatka and Ricles [22] in their study on 10-bay space truss. This study also takes into account statistical confidence factors for structural parameters and potential experimental instrumentation error. Capecchi and Vestroni [23] address the problem of understanding, when it is sufficient to measure and use only natural frequencies and avoiding mode shape measurements in damage detection problems. Farrar and Doebling [24] discuss application of damage detection methods that are based on changes in free vibration characteristics and also statistical pattern recognition tools to characterize damages to bridges and concrete columns.

In view of long-term health monitoring requirements of structures, such as bridges, it is desirable that the damage detection techniques must employ operating loads, such as vehicular loads, as excitation sources. There are a few studies which address the problem of modal testing and analysis of structures under operational loads [25–27]. The use of these studies to develop a procedure for detection of structural damages does not seem to have received wide attention. It must be emphasized that the success of damage detection procedures using vibration data requires that the in-built analytical procedures to be accurate enough to discern changes in response due to damages that could be small. This would mean that the analytical models employed here need to be more refined than what otherwise is needed in a routine response analysis. It is to be noted in this context that the bridge–vehicle system constitutes a time-varying system. Consequently, modal domain descriptors of bridge structure, such as natural frequencies, mode shapes, modal damping and frequency response function are not directly relevant to detect damages in such systems. Of course, if one ignores the vehicle structure interactions and treats the moving vehicle as a moving force, the system becomes time invariant in nature and, modal domain descriptors could still be used for damage detection purposes. In this case, however, the errors due to ignoring vehicle structure interactions would introduce unknown errors into damage detection procedures. In fact, it is not obvious on how modal information of bridge structures could be extracted based on measurement of vibration induced by vehicular traffic if one includes vehicle–structure interaction effects into the analysis. The focus of the present study is therefore to develop a time-domain approach to detect damages in bridge structures by analyzing the combined system of bridge and vehicle. The study assumes that the structural properties and motion characteristics of the moving vehicle are known. This assumption can be considered acceptable if the vehicle to be used in generating the test signal is a test vehicle whose structural properties are known before hand and it is driven with specified velocity and acceleration. The study combines finite element modelling for bridge vehicle system with a time-domain formulation to detect changes in structural parameters. Different damage scenarios, such as local/distributed loss of stiffness and bearings becoming partially immobile are examined. Questions on spatial incompleteness of measured data, influence of measurement noise and influence of bridge deck unevenness are also addressed. The feasibility of the procedures developed is demonstrated by using synthetic vibration data from damaged bridge models.

2. Finite element model for the bridge–vehicle system

We begin by considering the bridge–vehicle system shown in Fig. 1. The bridge deck is modelled approximately as a Euler–Bernoulli beam and the vehicle is modelled as a single d.o.f. system with sprung and unsprung masses. Furthermore, the bridge deck is assumed to possess a surface unevenness denoted by $r(x)$. The bridge, in its undamaged state, is taken to be simply supported and is allowed to have spatially varying flexural rigidity. The types of damages that are considered in this study include local/distributed loss of stiffness and the possibility of the bearings becoming partially immobile. The effect of partially immobile bearings is represented by a rotary spring at the ends as shown in Fig. 1. For the bridge in its undamaged state, the value of the rotary springs at the ends would be zero. The vehicle is assumed to travel with a velocity v and an acceleration a. The vehicle enters the bridge at $t = 0$ and exits the bridge at $t = t_f$. The structure is assumed to behave linearly and the vehicle is assumed to be in contact with the bridge deck at all times while it traverses the bridge. Under these assumptions, the governing equation of motion for the bridge–vehicle system, for $0 < t \leqslant t_f$, can be shown to be given by [28,29]

$$m_1\ddot{y} + c_1\left[\dot{y} - \frac{\mathrm{D}}{\mathrm{D}t}\left\{w\left(vt + \frac{1}{2}at^2, t\right) + r\left[vt + \frac{1}{2}at^2\right]\right\}\right] + k_1\left\{y - w\left(vt + \frac{1}{2}at^2, t\right)\right.$$
$$\left. - r\left[vt + \frac{1}{2}at^2\right]\right\} = 0, \tag{1}$$

$$\frac{\partial^2}{\partial x^2}\left[EI(x)\frac{\partial^2 w}{\partial x^2}\right] + m\frac{\partial^2 w}{\partial t^2} + c\frac{\partial w}{\partial t} = f(x,t)\delta\left(x - vt - \frac{1}{2}at^2\right), \tag{2}$$

$$f(x,t) = (m_1 + m_2)g + k_1[y(t) - w(x,t) - r[x(t)]] + c_1[\dot{y}(t) - \frac{\mathrm{D}}{\mathrm{D}t}\{w(x,t) + r[x(t)]\}]$$
$$-\ m_2\frac{\mathrm{D}^2}{\mathrm{D}t^2}\{w(x,t) + r[x(t)]\}. \tag{3}$$

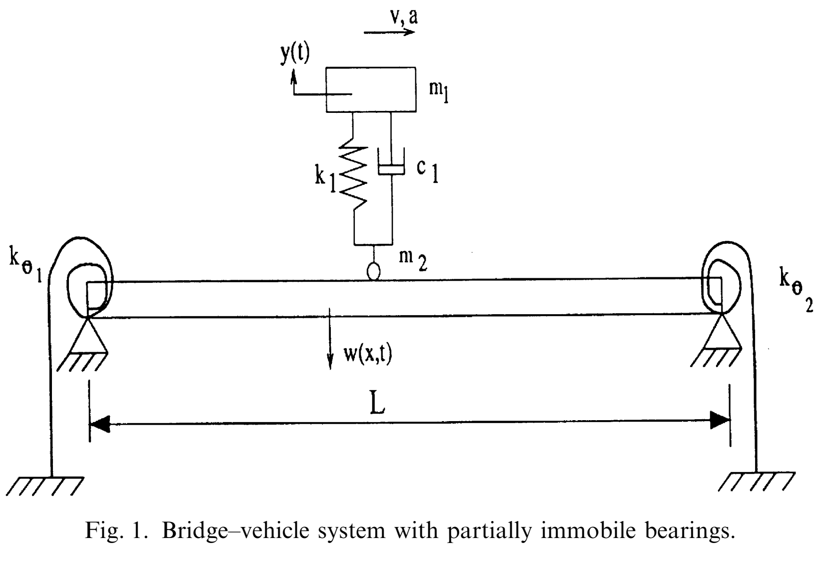

Fig. 1. Bridge–vehicle system with partially immobile bearings.

Here m_1, m_2, k_1, c_1 are vehicle parameters as shown in Fig. 1, $y(t)$ the vertical deflection of the vehicle sprung mass, $w(x,t)$ the transverse deflection of the beam, $EI(x)$ the flexural rigidity of the beam, m the mass per unit length of the beam, c the coefficient of viscous damping for the beam, g the acceleration due to gravity, and $\delta(\cdot)$ the Dirac's delta function. The total derivative $\mathrm{D}/\mathrm{D}t$ appearing in the above equations takes into account the Coriolis effect arising from the rolling of the vehicle mass on the deflected profile of the beam. The boundary conditions appropriate for the system shown in Fig. 1 reads

$$w(0,t)=0, \quad \frac{\partial}{\partial x}\left[EI(0)\frac{\partial^2 w(0,t)}{\partial x^2}\right]+k_{\theta 1}\frac{\partial w(0,t)}{\partial x}=0,$$
$$w(L,t)=0, \quad \frac{\partial}{\partial x}\left[EI(L)\frac{\partial^2 w(L,t)}{\partial x^2}\right]-k_{\theta 2}\frac{\partial w(L,t)}{\partial x}=0. \tag{4}$$

In the present study, we adopt the framework of finite element method to formulate the damage detection strategy. Accordingly, we begin by expressing the displacement field as

$$w(x,t)=[N(x)]\{d(t)\}. \tag{5}$$

Here $N(x)$ is the matrix of interpolation functions and $\{d(t)\}$ is the vector of nodal degrees of freedom associated with the beam nodes. Following the steps as outlined by Filho [29] the governing equation for the bridge–vehicle system for $0<t\leqslant t_f$ is obtained as

$$\begin{bmatrix}[M]+[m]^* & \{0\}\\ \{0\} & m_1\end{bmatrix}\begin{Bmatrix}\{\ddot{d}\}\\ \ddot{y}\end{Bmatrix}+\begin{bmatrix}[C]+[c]^* & -c_1[N]^{\mathrm{T}}\\ -c_1[N] & c_1\end{bmatrix}\begin{Bmatrix}\{\dot{d}\}\\ \dot{y}\end{Bmatrix}$$
$$+\begin{bmatrix}[K]+[k]^* & -k_1[N]^{\mathrm{T}}\\ -c_1[v+at][N]_x-k_1[N] & k_1\end{bmatrix}\begin{Bmatrix}\{d\}\\ y\end{Bmatrix}=\begin{Bmatrix}[N]^{\mathrm{T}}(m_1+m_2)g\\ 0\end{Bmatrix}, \tag{6}$$

where

$$[m]^*=m_2[N]^{\mathrm{T}}[N], \quad [c]^*=2m_2\dot{x}[N][N]_x+c[N]^{\mathrm{T}}[N],$$
$$[k]^*=m_2(v+at^2)^2[N]^{\mathrm{T}}[N]_{xx}+c(v+at)[N]^{\mathrm{T}}[N]_x+m_2[N]^{\mathrm{T}}[N]_x a_o+k_1[N]^{\mathrm{T}}[N]. \tag{7}$$

The superscript T in the above equations denotes the matrix transpose. The matrices M, C and K, respectively, denote the mass, damping and stiffness matrices of the beam structure. Furthermore, $[N]_x$ and $[N]_{xx}$, respectively, denote the first and the second derivative with respect to x of the matrix $[N]$. Upon the exit of the vehicle from the bridge, that is, for $t\geqslant t_f$, the governing equation of motion for the bridge reads

$$[M]\{\ddot{d}\}+[C]\{\dot{d}\}+[K]\{d\}=0. \tag{8}$$

The initial conditions for these equations, at $t=t_f$, are obtained from solution of Eq. (6) at $t=t_f$. It must be noted that the governing equations of motion, as given in Eq. (6), constitute a set of coupled linear ordinary differential equations with time-varying coefficients. Consequently, these equations cannot be uncoupled using the traditional normal mode expansions. It may be noted that the formulation of Eqs. (1)–(8) largely follows the approach outlined by earlier researchers [28,29].

3. Damage detection algorithm

Attention is focussed in the present study on two types of damage scenarios. Firstly, we assume that the flexural rigidity, EI_i, of the ith finite element of the beam, upon the occurrence of damage, becomes $\alpha_i EI_i$. Secondly, we consider the possibility of the bearings becoming partially immobile. This is modelled by emergence of rotary stiffnesses, represented by the springs with stiffness $k_{\theta 1}$ and $k_{\theta 2}$, (see Fig. 1) at the beam ends which otherwise are absent in an undamaged beam. The problem of damage detection thus can be stated as finding $(\alpha_i)_{i=1}^{n_e}$, $k_{\theta 1}$ and $k_{\theta 2}$ based on measurement of $y(t_j)$, $\dot{y}(t_j)$, $\ddot{y}(t_j)$, $\{d(t_j)\}$, $\{\dot{d}(t_j)\}$, and $\{\ddot{d}(t_j)\}$ for $j = 1, 2, \ldots, s$. Here n_e is the number of finite elements into which the beam structure is divided. Clearly, for the undamaged structure, $\alpha_i = 1$ for $i = 1, 2, \ldots, n_e$ and $k_{\theta 1}, k_{\theta 2} = 0$. Thus, any departure in the values of α_i, from the reference value of unity, and, in the values of $k_{\theta 1}$ and $k_{\theta 2}$, from the reference value of zero, indicates the occurrence of damage. It is also clear that the determination of these variables also helps to locate the damage and also to quantify its severity. It is assumed in the present study that the characteristics of the vehicle, namely, m_1, m_2, c_1, k_1 and its velocity and acceleration are known. It is also assumed that the bridge mass and damping matrices are unaffected by occurrence of the damage and hence are taken to be known a priori.

To describe the damage detection algorithm, we begin by considering the case of $k_{\theta 1} = k_{\theta 2} = 0$. The beam itself is taken to have undergone changes in its flexural rigidity. The stiffness matrix of the damaged beam structure is expressed in the form

$$K = \sum_{i=1}^{n_e} \alpha_i [A]_i^{\mathrm{T}} [\bar{K}]_i [A]_i. \tag{9}$$

Here $[\bar{K}]_i =$ the $n\text{-}d.o.f. \times n\text{-}d.o.f.$ stiffness matrix of the ith element in its undamaged state in the global co-ordinate system and $[A]_i =$the $n\text{-}d.o.f. \times n$ matrix of extended element nodal displacement that facilitates automatic assemblying of global stiffness matrix from the constituent element stiffness matrix. Based on the values of the beam and vehicle responses measured at $t = t_j$, Eq. (6) can be re-cast to read

$$[K]\{d(t_j)\} = \{F(t_j)\}, \tag{10}$$

where

$$\begin{aligned} F(t_j) = & -[[M] + [m(t_j)]^*]\{\ddot{d}(t_j)\} - [[C] + [c(t_j)]^*]\{\dot{d}(t_j)\} \\ & + c[N]^{\mathrm{T}}\{\dot{y}(t_j)\} - [k(t_j)]^*\{d(t_j)\} + k[N]^{\mathrm{T}}\{y(t_j)\} + (m_1 + m_2)g[N]^{\mathrm{T}}, \quad 0 < t \leqslant t_f, \end{aligned} \tag{11}$$

$$F(t_j) = -[M]\{\ddot{d}(t_j)\} - [C]\{\dot{d}(t_j)\} \quad t \geqslant t_f. \tag{12}$$

Using Eq. (9), Eq. (10) can be re-cast as

$$\sum_{i=1}^{n_e} \alpha_i \{B(t_j)\}_i = \{F(t_j)\}, \tag{13}$$

where $\{B(t_j)\}_i$ is a $n \times 1$ vector given by

$$\{B(t_j)\}_i = [A]_i^{\mathrm{T}}[K]_i[A]_i\{d(t_j)\}. \tag{14}$$

Eq. (13) can also be written as

$$\mathscr{B}(t_j)\{\alpha\} = \{F(t_j)\}, \tag{15}$$

where $\mathscr{B}(t_j)$ is a $n \times n_e$ matrix given by

$$\mathscr{B}(t_j) = [B_1(t_j)\ B_2(t_j)\cdots B_{n_e}(t_j)] \tag{16}$$

and $\{\alpha\}$ is a $n_e \times 1$ matrix of damage indicator factors. If response measurements are made for the time instants $t = t_1, t_2, \ldots, t_s$, equations governing α, as given by Eq. (15), can be written for each of these time instants. Consequently, one gets the set of equations

$$[\mathscr{L}]\{\alpha\} = \{\mathscr{F}\}, \tag{17}$$

where $[\mathscr{L}]$ is a $sn \times n_e$ matrix given by

$$[\mathscr{L}]^{\mathrm{T}} = [\mathscr{B}(t_1)\ \mathscr{B}(t_2)\cdots\mathscr{B}(t_s)] \tag{18}$$

and $\{\mathscr{F}\}$ is a $sn \times 1$ vector given by

$$\{\mathscr{F}\}^{\mathrm{T}} = [F(t_1)F(t_2)\cdots F(t_s)]. \tag{19}$$

Eq. (17) represents sn number of linear algebraic equations for the unknowns α_i, $i = 1, 2, \ldots, n_e$. These equations would most often be overdetermined and, consequently, an optimal solution can be obtained as

$$\{\alpha\} = [\mathscr{L}]^{+}\{\mathscr{F}\}. \tag{20}$$

Here $[\mathscr{L}]^{+}$ represents the left pseudo-inverse of the rectangular matrix and is given by

$$[\mathscr{L}]^{+} = [\mathscr{L}^{\mathrm{T}}\mathscr{L}]^{-1}\mathscr{L}^{\mathrm{T}}. \tag{21}$$

It is of significant interest to note that Eq. (17), governing the unknown $\{\alpha\}$, constitutes a set of *linear* algebraic equations. This fact is of significance, given that modal domain damage detection procedures invariably lead to non-linear equations for the damage parameters.

The above equations for the damage indicator factors α have been derived by assuming that $k_{\theta 1}, k_{\theta 2} = 0$. This would mean that the above procedure would not apply to detect the possibility of the bearings becoming partially immobile. In this context it must be noted that the damage indicator factor, α_i, essentially multiplies the stiffness parameter in the undamaged state to yield the corresponding stiffness parameter in the damaged state. Since, in the undamaged state $k_{\theta 1} = 0$ and $k_{\theta 2} = 0$, introducing a multiplying parameter to detect a non-zero $k_{\theta 1}$ and $k_{\theta 2}$ is clearly infeasible. To overcome this difficulty, the notion of a reference structure is introduced. This structure has two hypothetical rotary springs, with respective stiffnesses $k_{\theta 1}^{*}$ and $k_{\theta 2}^{*}$, attached to it at the two ends. To detect the possibility of bearings becoming partially immobile, two parameters α_l and α_r are introduced, such that, the bearing stiffness against rotation in the damaged state is given by

$$k_{\theta 1} = \alpha_l k^*_{\theta 1}, \quad k_{\theta 2} = \alpha_r k^*_{\theta 2}. \tag{22}$$

With this additional feature, the detection of damage can now be carried out using the steps as described in deriving Eq. (17). The damage indicator vector α in this case reads

$$\alpha = \{\alpha_1 = \alpha_l, \alpha_2, \ldots, \alpha_{n-1}, \alpha_n = \alpha_r\}. \tag{23}$$

Clearly, the estimates of α_l and α_r depend upon the values chosen for the reference parameters $k^*_{\theta 1}$ and $k^*_{\theta 2}$. To make an optimal choice, a non-dimensional quantity

$$\varepsilon(k^*_{\theta 1}, k^*_{\theta 2}) = \sum_{j=1}^{n} \sum_{i=1}^{s} \frac{\{d_j(t_i, k^*_{\theta 1}, k^*_{\theta 2}) - d_j^M(t_i)\}^2}{[d_j^M(t_i)]^2} \tag{24}$$

is introduced. Here $d_j(t_i, k^*_{\theta 1}, k^*_{\theta 2})$ is the estimated displacement at jth d.o.f. at $t = t_i$ with $k_{\theta 1} = k^*_{\theta 1}$, $k_{\theta 2} = k^*_{\theta 2}$ and $d_j^M(t_i)$ the measured response of the damaged structure at jth d.o.f. at time $t = t_i$. The best choice for $k^*_{\theta 1}$ and $k^*_{\theta 2}$ is taken to be the one that minimizes $\varepsilon(k^*_{\theta 1}, k^*_{\theta 2})$. This minimization itself could be carried out by conducting a parametric study on $\varepsilon(k^*_{\theta 1}, k^*_{\theta 2})$ by varying $k_{\theta 1}$ and $k_{\theta 2}$.

4. Problem of spatial incompleteness of measurements

The formulation presented in the previous section is based on the implicit assumption that it is possible to measure the response at all the d.o.f.'s considered in the finite element model. This clearly is an unrealistic assumption given that

- it is not easy to measure rotational d.o.f.'s,
- number of d.o.f.'s that could be measured simultaneously is limited by the number of channels available in the measurement set-up, and
- not all d.o.f.'s need be accessible for measurement.

The consequent difficulties arising out of these limitations could be addressed by adopting a model reduction scheme to approximate the d.o.f.'s that are not measured in terms of those that are measured. There exists several reduction schemes in the literature, such as, static and dynamic condensation techniques and system equivalent reduction and expansion process (SEREP), that could be used in this context [30,31]. To implement these schemes for the problem on hand, we assume that vehicle response $y(t)$ is measured and we designate all the beam d.o.f.'s that are measured as master d.o.f.'s and denote them by $d_m(t)$, and, the remaining beam d.o.f.'s are called the slave d.o.f.'s, and are denoted by $d_s(t)$. Thus, the beam d.o.f.'s are partitioned as

$$\{d(t)\}^{\mathrm{T}} = [\{d_m(t)\}\{d_s(t)\}]. \tag{25}$$

Accordingly, the bridge mass, stiffness and modal matrices also get partitioned as

$$K = \begin{bmatrix} K_{mm} & K_{ms} \\ K_{sm} & K_{ss} \end{bmatrix},$$
$$M = \begin{bmatrix} M_{mm} & M_{ms} \\ M_{sm} & M_{ss} \end{bmatrix},$$
$$[\Phi] = \begin{bmatrix} \Phi_m \\ \Phi_s \end{bmatrix}. \tag{26}$$

The reduction scheme here is proposed to be applied only to the beam d.o.f.'s. The essence of all the alternative reduction schemes is to introduce the transformation

$$\{d(t)\} = [W]\{d_m(t)\}. \tag{27}$$

Here $[W]$ is the $n \times n_m$ transformation matrix that relates the $n \times 1$ beam d.o.f.'s with the $n_m \times 1$ master d.o.f.'s. Eq. (27) can also be viewed as a model interpolation scheme to relate unmeasured d.o.f. to the measured d.o.f. If one adopts the static condensation technique, the transformation matrix can be shown to be given by

$$[W] = \begin{bmatrix} I \\ -K_{ss}^{-1}K_{sm} \end{bmatrix}. \tag{28}$$

Similarly, if one adopts the dynamic condensation technique for reduction, one gets

$$[W] = \begin{bmatrix} I \\ -D_{ss}^{-1}D_{sm} \end{bmatrix}. \tag{29}$$

Here, D is the dynamic stiffness matrix given by $D = [K - \omega^2 M]$ and ω is the frequency at which the reduction is made. Finally, if one adopts the SEREP for reduction, the transformation matrix reads

$$[W] = \begin{bmatrix} \Phi_m \\ \Phi_s \end{bmatrix} [\Phi_m^{\mathrm{T}}\Phi_m]^{-1}\Phi_m^{\mathrm{T}}. \tag{30}$$

In arriving at this transformation matrix, the displacement vector $\{d(t)\}$ is expressed in terms of the generalized co-ordinates $\{z(t)\}$ as $\{d(t)\} = [\Phi]\{z(t)\}$. Upon partitioning the displacement vector into master and slave d.o.f.'s, as in Eq. (25), and partitioning the modal matrix as in Eq. (26), it follows that $\{d_m(t)\} = [\Phi_m]\{z(t)\}$ and $\{d_s(t)\} = [\Phi_s]\{z(t)\}$. This leads to the expression for the generalized co-ordinate vector $\{z(t)\} = [\Phi_m]^{+}\{d_m\}$ where $[\Phi_m]^{+} = [\Phi_m^{\mathrm{T}}\Phi_m]^{-1}[\Phi_m]^{\mathrm{T}}$ is the pseudo-inverse of $[\Phi_m]$. This leads to the transformation matrix as given in Eq. (30). The relative merits of the above mentioned reduction schemes are widely discussed in the literature, see, for instance, Ref. [31]. The accuracy of static and dynamic condensation techniques is affected by the choice of active d.o.f.'s. On the other hand, SEREP provides features that the other two reduction schemes do not such as [31]:

- The arbitrary selection of modes that are to be preserved in the reduced system model.
- The quality of the reduced model is not dependent upon the location of the selected active d.o.f.

- The frequencies and the mode shapes of the reduced system are exactly equal to the frequencies and mode shapes (for the selected modes) of the full system model.

Upon the reducing the d.o.f.'s as indicated in Eq. (26), the reduced mass, stiffness and damping matrices for the beam structures are obtained as

$$[M_r] = [W]^T[M][W], \quad [K_r] = [W]^T[K][W], \quad [C_r] = [W]^T[C][W]. \tag{31}$$

In the damage detection procedure outlined in the previous section, we now need to use the above reduced matrices in place of the structural matrices $[M], [C]$ and $[K]$. Since the reduced matrices are dependent on the transformation matrix W, which, in turn, depends on the unknown structural stiffness matrix, the final set of equations governing the damage indicator vector α (Eq. (17)) becomes non-linear in nature. It is proposed in this study to solve these equations in an iterative manner. Here, in the first iteration, the transformation matrix W is derived by using the stiffness matrix that is valid for the undamaged structure. This leads to a first approximation of the damage indicator vector α. This is used to update the transformation matrix W and the process is repeated till satisfactory convergence on the elements of vector α is achieved. It is to be noted that the W matrix that would be eventually used in arriving at the converged α depends upon Φ matrix of the damaged structure.

5. Effect of measurement noise

Given that the measured response vector $\{d_m(t)y(t)\}^T$ is likely to be corrupted by measurement noise, it is of interest to determine the influence of this noise on the estimated damage indicator vector α. In our study, we model the measurement noise from different channels as a vector of zero mean, stationary, mutually independent, Gaussian random processes. Accordingly, the measured responses are now represented as

$$\{d_m(t)\} = \{d_{m0}(t)\} + \{\xi_d(t)\}, \tag{32}$$

$$\{y(t)\} = \{y_0(t)\} + \{\xi_y(t)\}. \tag{33}$$

Here the subscript zero indicates mean values and the vector $\{\xi_d(t)\}$ and the process $\{\xi_y(t)\}$ are, respectively, the measurement noise associated with bridge response and vehicle response. It follows that vector α is now a vector of random variables. In this study, a first order perturbation scheme is proposed to be employed to obtain approximations to the mean and covariance matrix of the vector α. Assuming the noise intensity to be small, and, using first order perturbation formalism, it can be shown that

$$\langle \alpha \rangle = \alpha_0, \tag{34}$$

$$\langle \alpha\alpha^T \rangle = [\mathscr{L}_o^+][\langle \Delta\mathscr{F}\Delta\mathscr{F}^T \rangle + \langle \Delta\mathscr{L}_o\mathscr{L}_o\Delta\mathscr{F}^T \rangle + \langle \Delta\mathscr{L}_o\mathscr{L}_o\mathscr{L}_o^T\Delta\mathscr{F}^T \rangle][\mathscr{L}_o^+]^T, \tag{35}$$

$$[\Delta\mathscr{L}_o]^T = [K_r\{\xi_d(t_1)\}, K_r\{\xi_d(t_2)\}, \ldots, K_r\{\xi_d(t_s)\}], \tag{36}$$

$$[\Delta\mathscr{F}]^T = [\Delta F(t_1)\Delta F(t_2)\cdots\Delta F(t_s)], \tag{37}$$

$$\Delta F(t_j) = [[M] + [m(t_j)]^*]\{\xi_d(t_j)\} + [[C] + [c(t_j)]^*]\{\dot{\xi}_d(t)\} + c_1[N]^{\mathrm{T}}\dot{\xi}_y(t_j) + k_1[N]^{\mathrm{T}}\xi_y(t_j) \quad (j = 1, 2, \ldots, s). \tag{38}$$

Here $\langle \cdot \rangle$ denotes the mathematical expectation operator and the quantities α_0 and $\mathscr{L}_o$ refer to the respective quantities when noise is absent. The expectations appearing on the right-hand of Eq. (34) can be expressed in terms of covariance matrix $\xi(t_j), \dot{\xi}(t_k)$ and $\ddot{\xi}(t_l), j, k, l = t_1, t_2, \ldots, t_s$. The evaluation of these expectations can be carried out by using standard theory of stationary random processes [32]. The details of these formulations are available in the thesis by Majumder [33].

6. Numerical results and discussions

To illustrate the formulations presented in the previous section, we consider the system shown in Fig. 1. It is assumed that the beam has uniform cross-sectional properties with $L = 45$ m, $EI = 1.62 \times 10^{11}$ N m^2, $m = 4625$ kg/m, $c = 1850$ N s/m. For the vehicle, it is assumed that $m_1 = m_2 = 500$ kg, $k_1 = 40 \times 10^7$ N/m and $c_1 = 160$ N s/m. The vehicle is assumed to travel with a velocity of 15 m/s and acceleration $a = 0$. The bridge deck unevenness $r(x)$ in the study is taken to be deterministic and, following the study by Honda et al. [34], $r(x)$ is taken to be a sample that is compatible with the power spectral density function given by

$$S_r(\Omega) = \frac{\bar{\alpha}}{\Omega^n + \beta^n}. \tag{39}$$

In the numerical work it is assumed that $\bar{\alpha} = 0.98 \times 10^{-4}$ m^2/m/cyc, $n = 1.92$, and $\beta = 0.06$ cyc/m. These parameters being representative of deck unevenness of girder-type bridges. The elements of noise vector $\{\xi_d(t)\}$ and $\{\xi_y(t)\}$ are taken to be a set of mutually independent band limited white processes spanning a frequency range of 2π–500π rad/s. The noise intensity was selected such that the standard deviation of the noise was about 1/30 of the peak bridge displacement in the absence of noise. The finite element model employed in this study for the bridge deck is as shown in Fig. 2. Here the bridge deck is divided in to 5 elements and each element is modelled as a Euler–Bernoulli beam. The model thus has 10 d.o.f.'s. The first three

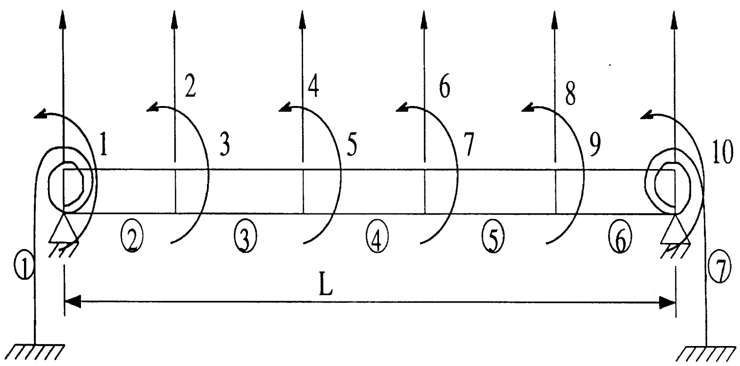

Fig. 2. Finite element model of the damaged bridge; numbers within circles indicate the element number.

natural frequencies of the bridge deck turn out to be 28.85, 115.57, 261.67 rad/s, respectively and, similarly, the vehicle natural frequency is 894.43 rad/s. The synthetic data for the damaged bridge response were obtained by integrating Eq. (6) using Newmark's-β method [30] with a step size of $\Delta t = 1.71 \times 10^{-4}$ s. Given the perceived merits of reduction scheme using SEREP, this method of reduction was employed in the damage detection algorithm. In all the instances when the reduction was carried out, the first four modes of vibration were retained and all rotational d.o.f.'s were treated as slave d.o.f.'s. Furthermore, as can be deduced from Eq. (17), the predicted value of α depends upon the length of observation made on the damaged structure response. In the numerical work, it was observed that the observation length of about $1.5t_f$ resulted in lowest level of errors in predicted α. Accordingly, an observation time of $1.5t_f$ has been used. It may be emphasized in this context, that the governing equations for the time interval $0 < t \leqslant t_f$ is given by Eq. (6) and for $t \geqslant t_f$ by Eq. (8). With a view to bring out different aspects of the formulation presented in the previous sections, the following investigations have been carried out.

Case A: We begin by considering measured response from an undamaged structure. The damage detection procedure in this case is expected to report no false alarms. The synthetic measured data, with all stiffness parameters fixed at their respective initial values, were inputed to the damage detection algorithm. The predicted damage vector, together with the details of error of detection, is reported in Table 1. The effect of using reduced set of measurements, that contains only displacement d.o.f.'s and the effect of possible presence of measurement noise are also studied in this table, see the first four rows in the table. In cases where the effect of noise is included, results on predicted mean as well as standard deviation of damage vector are included in this table (rows A.3 and A.4). Using criterion given in Eq. (24), it was found that, $k^*_{\theta_1} = k^*_{\theta_2} = 1.07 \times 10^{-7}$ N m/rad yielded minimum value for $\varepsilon(k^*_{\theta 1}, k^*_{\theta 2})$. A comparison of the predicted damage vectors (column 2) with the induced damage vectors (column 3) reveals that the damage detection algorithm performs satisfactory. The last column in this table reports the maximum percentage error between the induced damage vector and predicted mean damage vector. This

Table 1
Induced and predicted damage indicator vectors of an undamaged bridge

Sl. no.	Induced damage vector	Detected damage vector	Max error ($\epsilon_{\max}$)%
A.1	$\alpha^T = \{0,1,1,1,1,1,0\}$	$\alpha^T = \{0.0, 0.9959, 0.9980, 0.9956, 1.0011, 1.0032, 0.0\}$	0.4400
A.2	$\alpha^T = \{0,1,1,1,1,1,0\}$	$\alpha^T = \{0.0, 0.9924, 0.9980, 1.0001, 1.0039, 1.0095, 0.0\}$	0.9500
A.3	$\alpha^T = \{0,1,1,1,1,1,0\}$	$\langle\alpha\rangle^T = \{0.0, 0.9959, 0.9980, 0.9956, 1.0011, 1.0032, 0.0\}$	0.4400
		$\sigma_\alpha^T = \{0.0, 0.0234, 0.0916, 0.1263, 0.1142, 0.1189, 0.0\}$	
A.4	$\alpha^T = \{0,1,1,1,1,1,0\}$	$\langle\alpha\rangle^T = \{0.0, 0.9924, 0.9980, 1.0001, 1.0039, 1.0095, 0.0\}$	0.9500
		$\sigma_\alpha^T = \{0.0, 0.0297, 0.0916, 0.13693, 0.1202, 0.1191, 0.0\}$	
A.5	$\alpha^T = \{0,1,1,1,1,1,0\}$	$\alpha^T = \{0.0, 0.7916, 1.14, 1.309, 0.8328, 0.7654, 0.0\}$	30.9
A.6	$\alpha^T = \{0,1,1,1,1,1,0\}$	$\alpha^T = \{0.0, 0.7209, 1.01, 1.318, 0.8708, 0.6703, 0.0\}$	31.8

Case A.1—response at all d.o.f.'s measured, measurement is not noisy. Case A.2—response at 2,4,6,8 measured, measurement is not noisy. Case A.3—response at all d.o.f.'s measured, measurement is noisy. Case A.4—response at 2,4,6,8 measured, measurement is noisy. Case A.5—response at all d.o.f.'s measured, measurement is not noisy. Case A.6—response at 2,4,6,8 measured, measurement is not noisy. ($k^*_{\theta 1} = k^*_{\theta 2} = 1.83 \times 10^{-8}$ N m/rad.)

error is computed using

$$\epsilon_{max} = \max_{1 \leqslant i \leqslant n} \left(\frac{\alpha_i^I - \alpha_i^D}{\alpha_i^I} \right) \times 100, \quad (40)$$

where α_i^I is the ith induced damage parameter and α_i^D the ith detected damage parameter. It is observed that, even with a reduced analytical model in damage detection, the maximum error remains less than 1%. It may also be noted that for the assumed intensity of measurement noise the highest coefficient of variation in the predicted damage vector is about 0.1368. The 5th and 6th rows in Table 1 shows the results of damage detection that neglects the dynamic interaction between vehicle and the bridge. Here, in identifying the vector α, the moving vehicle was modelled as a moving force. The maximum error in the predicted damage vectors in this two cases is clearly seen to be much higher than those predicted in cases A.1–A.4. This clearly brings out the need for including bridge–vehicle interaction models for the problems considered in this paper.

Case B: The efficacy of the damage detection procedure, when the structure has suffered a local loss of stiffness is studied in Table 2. Two discrete damages are introduced into the model: firstly, the flexural rigidity of element 6 (Fig. 2) is reduced by 10% and, secondly, the left support bearing is taken to become partially immobile with resulting $k_{\theta 1} = 4.0 \times 10^{11}$ N m/rad. The results on predicted damage vector are shown in Table 2. The organization of this table is as in Table 1. In this case the maximum error in predicting damage is observed to occur when the measured d.o.f.'s include only d.o.f. 2 and 4 case (B.5). These d.o.f.'s, as may be seen from Fig. 2, are remotely placed from the location of damage. The magnitude of error in this case is 1.32% which can still be considered to be acceptably small. The smallness of errors observed in this case points towards the effectiveness of SEREP reduction scheme that is in-built into the damage detection algorithm.

Case C: The damage scenario assumed here involves a loss of stiffness in element 2 by 5%, and in element 6 by 10% and also both the bearings becoming partially immobile with $k_{\theta 1} = k_{\theta 2} = 4.0 \times 10^{11}$ N m/rad. Using criterion given in Eq. (24) it was found that the minimum value of $\varepsilon(k^*_{\theta 1}, k^*_{\theta 2})$ occured when $k^*_{\theta_1}$ and $k^*_{\theta 2}$ were in the neighbourhood of $k^*_{\theta 1} = 4.0 \times 10^{11}$ N m/rad. This

Table 2
The case of damage due to loss of local stiffness and one bearing becoming partially immobile

Sl. no.	Induced damage vector	Detected damage vector	Max error ($\epsilon_{\max}$)%
B.1	$\alpha^T = \{1, 1, 1, 1, 1, 0.9, 0.0\}$	$\alpha^T = \{0.9969, 0.9969, 0.9979, 0.9992, 1.0004, 0.8979, 0.0\}$	0.3081
B.2	$\alpha^T = \{1, 1, 1, 1, 1, 0.9, 0.0\}$	$\alpha^T = \{1.0054, 0.9962, 0.9927, 1.0026, 1.0030, 0.9051, 0.0\}$	0.7266
B.3	$\alpha^T = \{1, 1, 1, 1, 1, 0.9, 0.0\}$	$\langle\alpha\rangle^T = \{0.9969, 0.9969, 0.9979, 0.9992, 1.0004, 0.8979, 0.0\}$ $\sigma_\alpha^T = \{0.0521, 0.0234, 0.0782, 0.1014, 0.1142, 0.1189, 0.0\}$	0.3081
B.4	$\alpha^T = \{1, 1, 1, 1, 1, 0.9, 0.0\}$	$\langle\alpha\rangle^T = \{1.0054, 0.9962, 0.9927, 1.0026, 1.0030, 0.9051, 0.0\}$ $\sigma_\alpha^T = \{0.0374, 0.0563, 0.0921, 0.1363, 0.1142, 0.1189, 0.0\}$	0.7266
B.5	$\alpha^T = \{1, 1, 1, 1, 1, 0.9, 0.0\}$	$\langle\alpha\rangle^T = \{0.9954, 0.9925, 0.9956, 1.0012, 1.0132, 0.9064, 0.0\}$ $\sigma_\alpha^T = \{0.0491, 0.0443, 0.0916, 0.1123, 0.1381, 0.1187, 0.0\}$	1.320

Case B.1—response at all d.o.f.'s measured, measurement is not noisy. Case B.2—response at 2,4,6,8 measured, measurement is not noisy. Case B.3—response at all d.o.f.'s measured, measurement is noisy. Case B.4—response at 2,4,6,8 measured, measurement is noisy. Case B.5—response at 2,4 measured, measurement is noisy. ($k^*_{\theta 1} = 4.0 \times 10^{11}$ N m/rad, $k^*_{\theta 2} = 1.83 \times 10^{-8}$ N m/rad.)

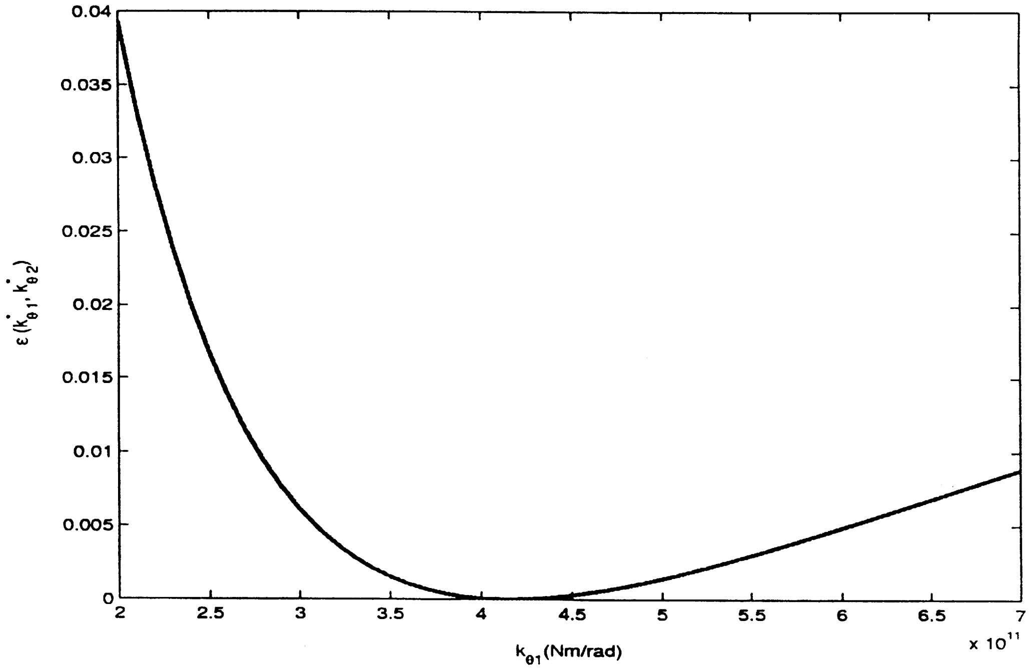

Fig. 3. Selection of $k^*_{\theta 1}$ and $k^*_{\theta 2}$ for case C (see Table 3); $\varepsilon(k^*_{\theta 1}, k^*_{\theta 2})$ is shown here along the line $k^*_{\theta 1} = k^*_{\theta 2}$.

Table 3
The case of damage detection using alternative reduction schemes and considering effect of deck unevenness

Sl. no.	Induced damage vector	Detected damage vector	Max error ϵ_{max}%
C.1	$\alpha^T = \{1, 0.95, 1, 1, 1, 0.9, 1\}$	$\alpha^T = \{0.9970, 0.9472, 0.9983, 0.9996, 1.0009, 0.9092, 1.0025\}$	0.2966
C.2	$\alpha^T = \{1, 0.95, 1, 1, 1, 0.9, 1\}$	$\alpha^T = \{0.9916, 0.9452, 1.0020, 1.0025, 1.0022, 0.9076, 0.9932\}$	0.8400
C.3	$\alpha^T = \{1, 0.95, 1, 1, 1, 0.9, 1\}$	$\langle\alpha\rangle^T = \{0.9970, 0.9472, 0.9983, 0.9996, 1.0009, 0.9092, 1.0025\}$ $\sigma^T_\alpha = \{0.0421, 0.0234, 0.0902, 0.1011, 0.1182, 0.1189, 0.0441\}$	0.2966
C.4	$\alpha^T = \{1, 0.95, 1, 1, 1, 0.9, 1\}$	$\langle\alpha\rangle^T = \{0.9916, 0.9452, 1.0020, 1.0025, 1.0022, 0.9076, 0.9932\}$ $\sigma^T_\alpha = \{0.0563, 0.0223, 0.0961, 0.1134, 0.1349, 0.1187, 0.732\}$	0.8400
C.5	$\alpha^T = \{1, 0.95, 1, 1, 1, 0.9, 1\}$	$\langle\alpha\rangle^T = \{0.9862, 0.9402, 0.9880, 0.9895, 0.9897, 0.9089, 0.9896\}$ $\sigma^T_\alpha = \{0.0413, 0.0223, 0.0805, 0.1134, 0.1427, 0.1091, 0.672\}$	1.3819
C.6	$\alpha^T = \{1, 0.95, 1, 1, 1, 0.9, 1\}$	$\alpha^T = \{1.0515, 0.943, 0.9974, 1.0071, 0.9955, 0.9147, 0.9814\}$	5.1476

Induced damage is due to distributed loss of stiffness and the two bearings becoming partially immobile. Case C.1—response at all d.o.f.'s measured, measurement is not noisy. Case C.2—response at 2,4,6,8 measured, measurement is not noisy. Case C.3—response at all d.o.f.'s measured, measurement is noisy. Case C.4—response at 2,4,6,8 measured, measurement is noisy. Case C.5—response at 2,4,6,8 measured, measurement is noisy and deck is uneven. Case C.6—response at 2,4,6,8 measured, measurement is not noisy and deck is smooth.

can be seen from Fig. 3 where $\varepsilon(k^*_{\theta 1}, k^*_{\theta 2})$, along the line $k^*_{\theta 1} = k^*_{\theta_2}$ is shown as a function of $k^*_{\theta 1}$. Accordingly, it was assumed in detecting damage that $k^*_{\theta 1} = k^*_{\theta 2} = 4.0 \times 10^{11}$ N m/rad. The results shown in the 5th row (case C.5) correspond to the case that includes the effect of deck unevenness in the measured response. The error of damage detection in this case marginally increases to 1.38% from a value of 0.84%, that occurs when bridge deck is smooth (case C.2). The last row in Table 3 illustrates predicted damage vector when Guyan's reduction scheme is employed for model reduction. The error of damage detection in this case becomes greater than 5% which is substantially higher than errors that occur when SEREP is used for reduction.

7. Assumptions and limitations of the present study

1. The damage scenarios studied in this paper are limited to localized/distributed loss of stiffness. While these scenarios might be illustrative of idealizations of damages due to discrete cracking or loss of pre-stress in pre-stressed concrete girders, further work is needed to model the damages more realistically. Specifically it is of interest to detect changes in mass and damping properties of the structure caused due to occurrence of damage. The treatment of changes to damping perhaps need to be treated probabilistically given the wide variations that occurs in characterization of damping.
2. The method has been illustrated using numerically simulated data from theoretical models. Although these data have been seeded with random noise, there is bound to exist differences between such artificial data and experimental/field data. In a field study, additional complications due to environmental effects such as those caused due to wind and temperature fluctuations would arise. Furthermore, there are going to exist other sources of uncertainty, such as intrinsic uncertainty associated with structural and vehicular properties, uncertainties associated with guideway uneveness and modelling uncertainty associated with structural modelling and vehicle–structure system and model reduction adopted in the study. Further work is needed to develop the proposed approach to incorporate these features so that the approach becomes practically applicable. Some of the recent studies on Bayesian methods for structural damage detection and model updating by Beck and Katafygiotis [35], Katafygiotis et al. [36], and Yuen and Katafygiotis [37] are likely to be of relevance in advancing the scope of the present study.
3. The proposed procedure has been illustrated with reference to a highly idealized beam-moving oscillator system. Treatment of real-life bridge–vehicle systems would require more elaborate finite element models for both the bridge and the vehicle. It may be noted that the form of the finite element equilibrium equations, as outlined in Eqs. (6)–(8), would remain broadly valid even for these more general applications. Consequently, the damage detection algorithm outlined in Section 2 remains applicable for these situations also.
4. The present study assumes that, upon the occurrence of damage, the structure continues to behave linearly. This assumption could be relaxed by adopting a non-linear finite element model for the structure. The damage detection algorithm would consequently become non-linear in nature. An initial effort to address this problem is reported in the paper by Majumder and Manohar [38].
5. The method proposed in this study requires measurements to be made on the moving vehicle also. This necessitates the use of an instrumented vehicle to generate the test signals to set the bridge into vibration. From an application point of view, it is desirable to eliminate this requirement. The present authors are currently exploring a study aimed at achieving this by using model reduction strategies.

8. Concluding remarks

A time-domain approach, within the framework of finite element modelling, has been developed in this study to detect damages in bridge structures using data on vibration induced by a moving vehicle. In studies of this kind it is important to recognize that the accuracy of damage detection crucially depends upon the ability of finite element model employed to capture changes in structural response caused due to damages. This calls for greater sophistication in finite element modelling than what perhaps is needed in problems of response prediction. The study reported in this paper accounts for several complicating features associated with response of bridge–vehicle system. This includes the effects due to dynamic interaction between vehicle and bridge, spatial incompleteness of measured data, deck unevenness and presence of measurement noise. The governing equations of motion in this case constitutes a set of coupled linear differential equation with time-varying coefficients. Consequently, the damage detection problem is not amenable for solution using modal domain techniques. The time-domain approach developed in this study leads to a set of overdetermined linear algebraic equations for the damage indicator variables which are solved using pseudo-inverse theory. The limited set of numerical illustrations reported in this paper demonstrates the accuracy of the method developed. Using the procedures recommended in this study, the maximum error that is found to occur in detection of damage is seen to remain less than about 1.5% for all the cases reported in this investigation.

Acknowledgements

The work reported in this paper has been supported by funding from the Council for Scientific and Industrial Research, Government of India.

References

[1] M.I. Friswell, J.E. Mottershead, Finite Element Model Updating in Structural Dynamics, Kluwer Academic Publishers, Dordrecht, 1996.
[2] C.R. Farrar, W. Scott, S.W. Doebling, A.N. David, Vibration-based structural damage identification, Philosophical Transactions of Royal Society London 359 (2001) 131–149.
[3] S.W. Doebling, C.R. Farrar, M.B. Prime, A summary review of vibration-based damage identification methods, Shock and Vibration Digest 30 (2) (1998) 91–105.
[4] S.W. Doebling, C.R. Farrar, M.B. Prime, D.W. Shevitz, Damage identification and health monitoring of structural and mechanical systems from changes in their vibration characteristics; a literature review, LA-13070-MS,UC-900, Los Alamos National Laboratory, Los Alamos, NM, 1996.
[5] J. He, Damage detection and evaluation I, in: J.M.M. Silva, N.M.M. Maia (Eds.), A Chapter in Modal Analysis and Testing, Kluwer Academic Publishers, Dordrecht, 1999, pp. 325–344.
[6] O.S. Salawu, Detection of structural damage through changes in frequency: a review, Engineering Structures 19 (9) (1997) 718–723.
[7] W.J. Staszewski, Structural and mechanical damage detection using wavelets, The Shock and Vibration Digest 30 (6) (1998) 457–472.
[8] D.F. Mazurek, J.T. Dewolf, Experimental study of bridge monitoring technique, Journal of Structural Engineering American Society of Chemical Engineers 115 (9) (1990) 2532–2549.

[9] G. Hearn, R.B. Testa, Modal analysis for damage detection in structures, Journal of Structural Engineering American Society of Chemical Engineers 117 (10) (1991) 3042–3063.
[10] G.C. Yao, K.C. Chang, G.C. Lee, Damage diagnosis of steel frames using vibrational signature analysis, Journal of Engineering Mechanics American Society of Chemical Engineers 118 (9) (1992) 1949–1961.
[11] S. Alampalli, G. Fu, Remote monitoring systems for bridge condition, Client Report 94, Transportation Research and Development Bureau, New York State Department of Transportation, 1994.
[12] S. Alampalli, G. Fu, E.W. Dillon, Measuring bridge vibration for detection of structural damage, Research Report 165, Transportation Research and Development Bureau, New York State Department of Transportation, 1995.
[13] J.R. Casas, A.C. Aparicio, Structural damage detection from dynamic test data, Journal of Structural Engineering American Society of Chemical Engineers 120 (8) (1994) 2437–2450.
[14] C.G. Koh, Damage detection of buildings: numerical and experimental studies, Journal of Structural Engineering American Society of Chemical Engineers 121 (8) (1995) 1155–1160.
[15] P.L. Liu, Identification and damage detection of trusses using modal data, Journal of Structural Engineering American Society of Chemical Engineers 121 (4) (1995) 599–608.
[16] H.L. Chen, C.C. Spyrakos, G. Venkatesh, Evaluating structural deterioration by dynamic response, Journal of Structural Engineering American Society of Chemical Engineers 121 (8) (1995) 1197–1204.
[17] S.S. Law, H.S. Ward, G.B. Shi, R.Z. Chen, P. Waldron, C. Taylor, Dynamic assessment of bridge load-carrying capacities I, Journal of Structural Engineering American Society of Chemical Engineers 121 (3) (1995) 478–487.
[18] S.S. Law, H.S. Ward, G.B. Shi, R.Z. Chen, P. Waldron, C. Taylor, Dynamic assessment of bridge load-carrying capacities II, Journal of Structural Engineering American Society of Chemical Engineers 121 (3) (1995) 488–495.
[19] K.G. Topole, N. Stubbs, Non-destructive damage evaluation of a structure from limited modal parameters, Earthquake Engineering and Structural Dynamics 24 (1995) 1427–1436.
[20] O.S. Salawu, C. Williams, Bridge assessment using forced-vibration testing, Journal of Structural Engineering American Society of Chemical Engineers 121 (2) (1995) 161–173.
[21] M.M. Waheb, G.D. Roeck, Dynamic testing of prestressed concrete bridges and numerical verification, Journal of Structural Engineering American Society of Chemical Engineers 3 (4) (1998) 159–169.
[22] J. Kosmatka, J.M. Ricles, Damage detection in structural modal vibration characterization, Journal of Structural Engineering American Society of Chemical Engineers 125 (12) (1999) 1384–1392.
[23] D. Capecchi, F. Vestroni, Monitoring of structural systems by using frequency data, Earthquake Engineering and Structural Dynamics 28 (1999) 447–461.
[24] C.R. Farrar, S.W. Doebling, Damage detection and evaluation II, in: J.M.M. Silva, N.M.M. Maia (Eds.), A Chapter in Modal Analysis and Testing, Kluwer Academic Publishers, Dordrecht, 1999, pp. 345–378.
[25] D. Wang, A. Haldar, Element-level system identification with unknown input, Journal of Engineering Mechanics American Society of Chemical Engineers 120 (1) (1994) 159–176.
[26] L.U.C. Hermans, H.V.D. Auweraer, Extraction and validation of structural models from tests under operational conditions, Proceedings of Symposium on International Automotive Technology, SIAT/SAE Technical Paper Series, Pune, India, 1999, pp. 293–302.
[27] S. Alampalli, T.G.H. Cioara, Selective random decrement technique for processing bridge vibration data, in: S. Alampalli (Ed.), Proceedings of Conference on Structural Materials Technology IV, Technomic Publishers, Lancaster, 2000, pp. 75–80.
[28] L. Fryba, Vibration of Solids and Structures under Moving Loads, Thomas Telford Publishing House, Prague, 1999.
[29] F.V. Filho, Finite element analysis of structures under moving loads, Shock and Vibration Digest 10 (1978) 27–35.
[30] A.K. Chopra, Dynamics of Structures, Prentice-Hall, Englewood Cliffs, NJ, 1996.
[31] J.O. Callahan, P. Avitable, R. Riemer, System equivalent reduction expansion process (SEREP), Proceedings of the Seventh International Modal Analysis Conference, Las Vegas, Nevada, February 29–37, 1989.
[32] A. Papoulis, Probability, Random Variables, and Stochastic Processes, 3rd Edition, McGraw-Hill, New York, 1991.
[33] L. Majumder, Bridge Damage Detection Using Ambient Vibration Data, M.Sc(Engg) Thesis, Indian Institute of Science, Bangalore, India, 2001.

[34] H. Honda, Y. Kajikawa, T. Kobori, Spectra of road surface roughness on bridges, Journal of Structures Division American Society of Chemical Engineers 108 (ST9) (1982) 1956–1966.
[35] J.L. Beck, L.S. Katafygiotis, Updating models and their uncertainties. I: Bayesian statistical framework, Journal of Engineering Mechanics 124 (4) (1998) 455–467.
[36] L.S. Katafygiotis, K.V. Yuen, J.C. Chen, Bayesian modal updating by use of ambient data, American Institute of Aeronautics and Astronautics Journal 39 (2) (2001) 271–278.
[37] K.V.Yuen, L.S. Katafygiotis, Bayesian modal updating using complete input and incomplete noisy measurements, Journal of Engineering Mechanics 128 (3) (2002) 340–350.
[38] L. Majumder, C.S. Manohar, Computers and Structures Nonlinear reduced models for beam damage detection using data on moving oscillator-beam interactions, under review.